Turbulent heat transfer and nanofluid flow in a pipe with half circle ribs

Hussein Togun*
*Head of Biomedical Engineering Department, University of Thi-Qar, 64001 Nassiriya, Iraq
*Corresponding author: htokan_2004@yahoo.com
Phone No: +9647829318426

Abstract: - Heat transfer and turbulent nanofluid flow in a pipe with half circle ribs are numerically examined. A finite volume method (FVM) based on shear-stress transport (SST) k-ω turbulence model are adopted. The Computational problem is solved for alumina–water (Al2O3-H2O) nanofluid ranged from 1% to 4%, turbulent regime Re = 10000 - 25000, step heights of ribs was 2.5mm and 5mm for pitch ratio changed from 5 to 40. The numerical results indicated that the effects of Reynolds number, steps height, and pitch ratio of ribs on enhancement of heat transfer. Increase of volume fraction of Al2O3 nanofluids leads to increases in local heat transfer coefficient and the highest local heat transfer coefficient observed with 4% volume fraction of Al2O3 nanofluids compared with others. It is also found that local pressure drop rises with Reynolds number and volume fraction of Al2O3 nanofluids due to increases in flow rate and density of conventional fluid. Recirculation flow observed after and before each rib which have major effect on thermal performance.

Key-Words: - Nanofluids, Augmentation heat transfer, Ribs channel, Recirculation flow, Turbulent flow

Nomenclature

Cp	Specific heat, J/kg k
dp	Diameter of nanofluid particles (nm)
df	Diameter of a base fluid molecule
H	Diameter of pipe, m
h	Rib height, m
Nu	Nusselt number
P	Pitch space , m
P/W	Pitch ratio
Pr	Prandtl number
Re	Reynolds number
T	Temperature, K
u, v	Axial velocity
W	Rib width, m
x, y	Cartesian coordinates, m

Greek symbols

δ	Kronecher delta function
μ	Dynamic viscosity. Pa s
μeff	Effective dynamic viscosity
ρ	Density, kg/m3
σ	Turbulent Prandtl number
τ	Wall shear stress, kg/m2
ω	Rate of dissipated turbulent kinetic energy
ϕ	Volume fraction (%)

1 Introduction

In recent years, the request of energy is increasing day by day with decreasing in resources of nonreplenishable energy. Many techniques are applied to improve the thermal performance in heat exchanging equipment, among them, use of efficient materials, regulating process factors, modifications of design etc. Currently, the studies are further included in exploration of enhanced heat exchanging fluid where nanofluids are receiving importance as heat exchanging liquid compared to conventional liquid.

Durst et al. [1] presented study of turbulent fluid flow of channel over two fences in tandem numerically and experimentally. The results showed that the effects of Reynolds number and blockage ratio on size and location of the primary and secondary recirculation zones. Heat transfer and pressure drop in a square channel with parallel, crossed and V-shaped angled ribs studied by Han et al. [2]. Nine rib shapes were concerned: 90º rib, 60º and 45º parallel ribs, 60 and 45ºcrossed ribs, 60 and 45º ∨-shaped ribs, and 60 and 45º ∧-shaped ribs. Highest heat transfer improvement observed at ∨-shaped rib while the maximum pressure drop occurred at ∧-shaped rib compared with others. Tanda [3] presented numerically and experimentally studied on heat transfer and fluid flow in rectangular channels with transverse and v shaped at angle of 45º or 60º. The maximum heat transfer enhancement found at v- broken ribs compared to the continuous ribs. Smulsky et al. [4] also conducted experimentally studied on heat transfer and separated flow through the channel with different orientation of ribs varied from 50° to 90°. Highest local heat transfer coefficient was about 40% at 50° bigger than 90°. Impinging jet array heat transfer from a surface with V-shaped and convergent divergent ribs experimental studied by Caliskan and Baskaya [5]. The augmentation of heat transfer was varied from 4% to 26% for V-SR arrangement compared to the smooth plate

Air flow and heat transfer in canal with half circle ribs numerically investigated by Hussein et al. [6] where SST k-ω turbulence Model used in their simulation. The findings leads to increase in heat transfer coefficient occurred at increase both Reynolds number and number of ribs. While Tuqa et al. [7] have numerical simulation on fluid flow and heat transfer in a duct with triangular ribs where seen that the highest thermal enhancement occurred at triangular ribs of angel 60° with Reynolds number of 60000 compared to ribs angle of 90° and 45°.

For more enhancement nanofluid used due to high specific surface area and therefore further heat transfer surface between particles and fluid. Therefore there some researchers concerned increase heat transfer by geometrical modifications and using nanofluids such as Hussein et al. [8-10], and Safeai et al., [11].

Fathinia et al. [12] performed numerical study on turbulent heat transfer and nanofluid flow in a channel over periodic grooves where used different types of nanoparticles as represented by SiO2, Al2O3, and ZnO, with volume fraction varied from 1% to 4%. The thermal performance was about 114% for SiO2 compared to the water in a grooved channel.

Nanofluid flow and heat transfer in ribbed channel numerically studied by Oronzio et al. [13] where seen that the more augmentation of thermal performance happens with using nanofluids through ribbed channel. Mohammed et al. [14] have numerically study on thermal and hydraulic characteristics of turbulent nanofluids flow in a rib–groove channel. In their study, four different types of nanoparticles Al2O3, CuO, SiO2, and ZnO for volume fractions varied from 1% to 4% and different base fluids. It can be seen that increase in volume fraction, Reynolds number, and aspect ratio effect on Nusselt number. They found that the increase in the Nusselt number with. The results showed that the maximum thermal performance obtained with rectangular rib–triangular groove and SiO2 nanofluid compared with others.

Aim of the present study is to investigate the effects of step height and pitch ratio of the ribs on thermal performance as well as effects of volume fraction of alumina–water (Al_2O_3-H_2O) nanofluid and Reynolds number are considered.

2 Mathematical model

2.1 Problem statement

The pipe configuration with half circle rib is presented schematically in Fig. 1. The dimensions of the pipe were 1000 mm length and 40 mm diameter while the dimensions of half circle ribs on wall were step height of 2.5 mm and 5mm, width changed from 5mm to 10 mm, pitch ratio (P/W) changed from 10 to 40 for 2.5mm rib height, 5 to 20 for 5 mm rib height, for more details see Table 1. Volume fraction of Al2O3 nanofluids was varied between 1% to 4% with water as a base fluid. The range of flow Reynolds number varied between 10000 to 25,000 at constant wall temperature of 320 K

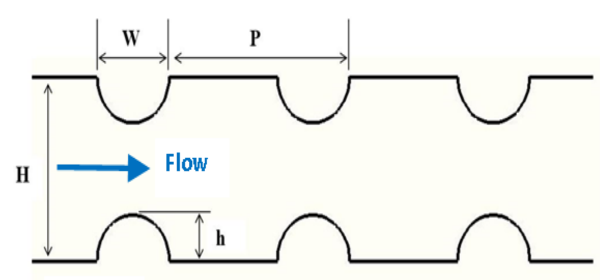

Fig. 1 Schematic diagram of a channel with half circle ribs

Table1: Dimensions of rib for six cases.

Case	h	h/H	P	P/W
1	2.5	0.06	50	10
2	2.5	0.06	100	20
3	2.5	0.06	200	40
4	5	0.12	50	5
5	5	0.12	100	10
6	5	0.12	200	20

2.2 Governing equations

FVM with Continuity, momentum, and energy equations with are applied in this simulation. Two dimensional domains, turbulent flow, steady state, and the working fluid is pure water and Al2O3 nanofluids. The shear-stress transport (SST) k-ω turbulence Model was adopted to solve the Navier stokes equations (1-6).

$$\frac{\partial}{\partial x_i}(\rho u_i) = 0 \qquad (1)$$

$$\frac{\partial}{\partial x_j}(\rho u_i u_j) = -\frac{\partial P}{\partial x_i} + \frac{\partial}{\partial x_i}\left[\mu\left(\frac{\partial u_i}{\partial x_j} + \frac{\partial u_j}{\partial x_i} - \frac{2}{3}\delta_{ij}\frac{\partial u_i}{\partial x_j}\right)\right] + \frac{\partial}{\partial x_j}\left(-\rho\overline{u_i' u_j'}\right) \qquad (2)$$

$$\frac{\partial}{\partial x_i}[u_i(\rho E + P)] = \frac{\partial}{\partial x_j}\left[\left(\lambda + \frac{c_p \mu_t}{Pr_t}\right)\frac{\partial T}{\partial x_j} + u_i(\tau_{ij})_{eff}\right] \qquad (3)$$

where

$$-\rho\overline{u_i' u_j'} = \mu_t\left(\frac{\partial u_j}{\partial x_i} + \frac{\partial u_i}{\partial x_j}\right) - \frac{2}{3}k\delta_{ij} \qquad (4)$$

The SST k-ω turbulence Model is represented by the two transport equations (5-6).

$$\frac{\partial}{\partial x_i}(\rho k u_i) = \frac{\partial}{\partial x_j}\left(\Gamma_k \frac{\partial k}{\partial x_j}\right) + G_k - Y_k \qquad (5$$

$$\frac{\partial}{\partial x_i}(\rho \omega k u_i) = \frac{\partial}{\partial x_j}\left(\Gamma_\omega \frac{\partial \omega}{\partial x_j}\right) + G_\omega - Y_\omega + D_\omega \qquad (6)$$

3 Numerical procedure

The governing equations have been discretized by a finite volume method within the computational domain [15, 16] based on considered boundary conditions. Second Order Central Difference and Second Order Upwind differencing were used to estimate the all terms in equations. The velocity-pressure coupled equation is solved by using SIMPLE algorithm [17,18]. Non-uniform (unstructured) grids were employed for meshing the solution domain. Increase mesh elements density near the ribs of the pipe for obtains high accuracy in numerical simulation.

In this simulation compute the residual sum for each variable and sorted after each iteration, hence saving the convergence history. The convergence criterion was less than 10^{-5} for continuity, and smaller than 10^{-6} for the momentum and smaller than 10-8 energy equations.

3.1 Grid Independent study and code validation

Three sizes of meshing are used in order to obtain grid independent and compared the results for pure water at the boundary condition of h/H= 0.12, p/w= 10, and Re= 10000 where observed a little different in value of average heat transfer coefficient between second and third grids then considered second grid as a grid independent as shown in Table 2.

Due to experimental data for heat transfer and turbulent nanofluids flow through the pipe with half circle ribs has not been investigated in the available literature, for validation of the current model, the numerical results for air flow through the pipe with semicircle ribs presented by Hussein et a. [6] are used. The current model applied using water for same geometry which studied by Hussein et a. [6] at Re =25000. It is observed that same trends for local heat transfer coefficient between current study and Hussein et al. [6] as shown in Fig. 2.

Table 2: Grid independent

No. of grid	node	h_{ave}
1	40480	1457.51
2	92400	1559.57
3	165760	1602.178

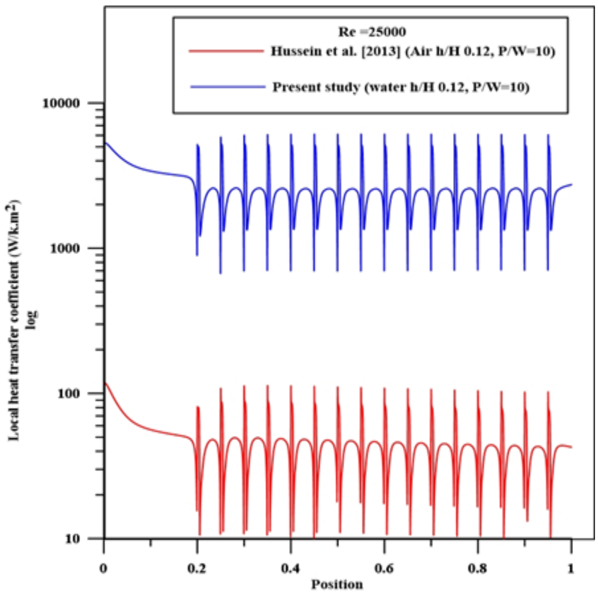

Fig.2 Comparison of trend of local heat transfer coefficient with Hussein et el. [2013].

4 Thermophysical properties of the nanofluid

Thermophysical properties of the nanofluid are computed by particular correlations. The effective density of nanofluid is reported as [19]

$$\rho_{nf} = (1-\phi)\rho_f + \phi\rho_{np} \qquad (7)$$

where ρ_f and ρ_{np} are term the density of base fluid and the solid nanoparticles , respectively.

The heat capacity of the nanofluid is presented by [19]

$$(\rho C_p)_{nf} = (1-\phi)(\rho C_p)_f + \phi(\rho C_p)_{np} \quad (8)$$

where $(\rho C_p)_f$ and $(\rho C_p)_{np}$ are define the heat capacities of the base fluid and the nanoparticles, respectively.

As observed by Koo and Kleinstreuer [20], the effective of thermal conductivity of nanofluid involves of static and Brownian effects, and could be computed with the following empirical correlations:

$$K_{eff} = K_{static} + K_{Brownian} \quad (9)$$

$$K_{static} = K_f\left[\frac{(K_{np}+2K_f)-2\phi(K_f-K_{np})}{(K_{np}+2K_f)+\phi(K_f+K_{np})}\right] \quad (10)$$

$$K_{Brownian} = 5\times10^4\beta\phi\rho_f C_{p,f}\sqrt{\frac{KT}{2\rho_{np}d_p}}f(T,\phi) \quad (11)$$

where k= 1.3809×10^{-23}J/K is the Boltzmann constant, and β is given as:

$$\beta = 8.4407(100\phi)^{-1.07304} \quad (12)$$

and $f(T,\phi)$ is given as

$$f(T,\phi) = (2.8217\times10^{-2}\phi + 3.917\times 10-3TT°+(-3.0669\times10-2\phi-3.91123\times10-3) \quad (13)$$

The effective dynamic viscosity for the nanofluid could be computed by using the following equations (Corcion [22]):

$$\mu_{eff} = \mu_f \times \frac{1}{(1-34.87(d_p/d_f)^{-0.3}*\phi^{1.03})} \quad (14)$$

$$d_f = \left(\frac{6M}{N\pi\rho_{f0}}\right)^{1/3} \quad (15)$$

where d_p and d_f are defined the diameter of the nanoparticles and equal diameter of a base fluid molecule , respectively; M is defined the molecular weight; N is represented the Avogadro number = 6.022×10^{23}mol^{-1}; and ρ_{f0} is the density of the base fluid found at Temperature=293K.

Table 3 shows the thermophysical properties of the nanofluid [21] and water [22].

The Nusselt number is defined as:

$$Nu = \frac{hd}{k} \quad (16)$$

where h is the heat transfer coefficient.

Table3:Thermophysical properties of nanoparticles (Al2O3) and water at T = 300 K.

Thermophysical properties	Al_2O_3 [21]	Water [22]
ρ (kg/m^3)	3600	996.5
Cp (J/kg k)	765	4181
K (W/m k)	36	0.613
μ (Ns/m^2)	-	1E-03

5 Results and discussion

5.1 Effect of Reynolds number

Different local heat transfer coefficient with Reynolds number at step height of 5 mm for pitch ratios (P/W) of 10 and 5 are presented in Figure 3 and 4, respectively. It can be seen that increase in heat transfer coefficient with increased Reynolds number for all cases due to increase the turbulent and recirculation flow through the flow channel. Generally, the higher local heat transfer coefficient noticed with greater Reynolds number.

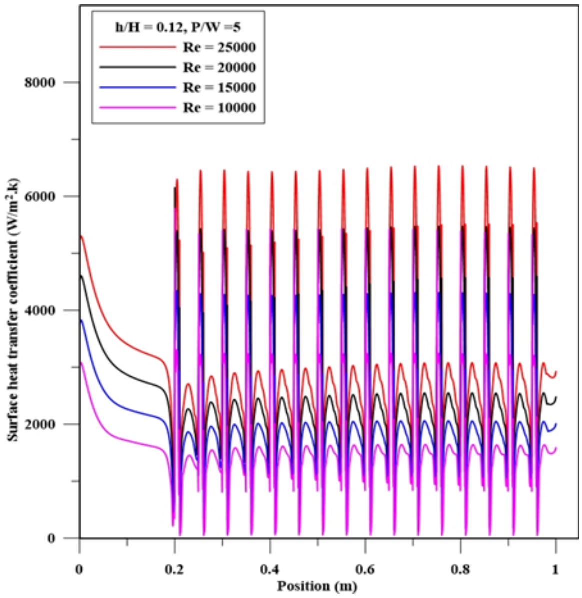

Fig. 3: Effect of Reynolds number on local heat transfer coefficient for h/H=0.12 and P/W=5.

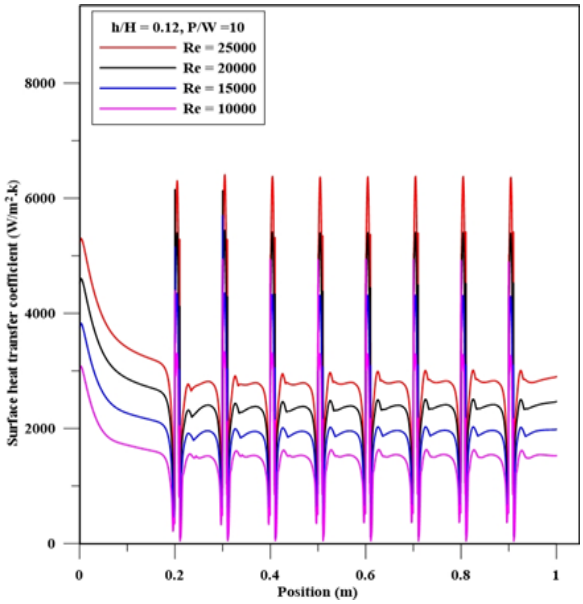

Fig. 4: Effect of Reynolds number on local heat transfer coefficient for h/H=0.12 and P/W=10.

5.2 Effect of pitch ratio

Figures 5 and 6 show differences of local heat transfer coefficient with pitch ratios (P/W) at step height ratios (h/H) 0.06 and 0.12 for Re = 25000, respectively. Augmentation of local heat transfer coefficient can be seen clearly with decreased of pitch ratio for all cases and that is because decrease pitch ratio leads to increase of number ribs where the number of peak in profile of local heat transfer coefficient represented the number ribs which induced turbulent augmentation heat transfer.

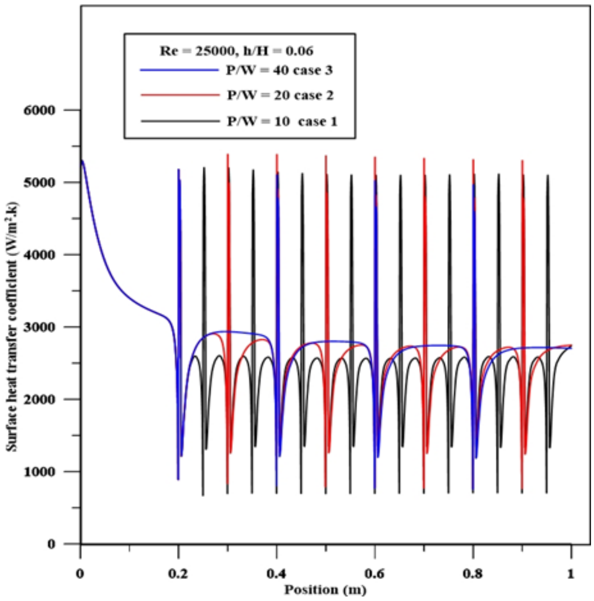

Fig. 5: Effect of pitch ratio on local heat transfer coefficient for h/H=0.06 at Re=25000

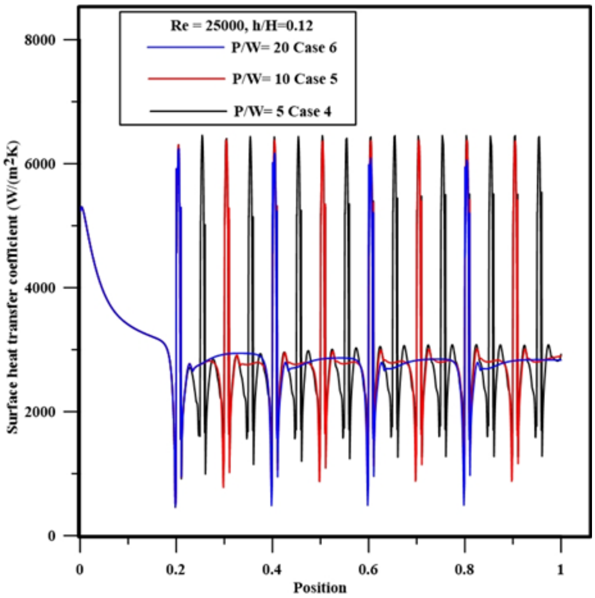

Fig. 6: Effect of pitch ratio on local heat transfer coefficient for h/H=0.12 at Re=25000.

5.3 Effect volume fraction of Nanofluids

Effect volume fraction of Al2O3 nanofluids on local heat transfer coefficient at Reynolds number of 25000 for pitch ratio of 10 and step height ratio of 0.12 are presented in Figure 7. The results show that increase volume fraction of Al2O3 nanofluids producing increase in heat transfer coefficient and the maximum value of heat transfer coefficient found at 4% volume fraction of Al2O3 nanofluids compared with others.

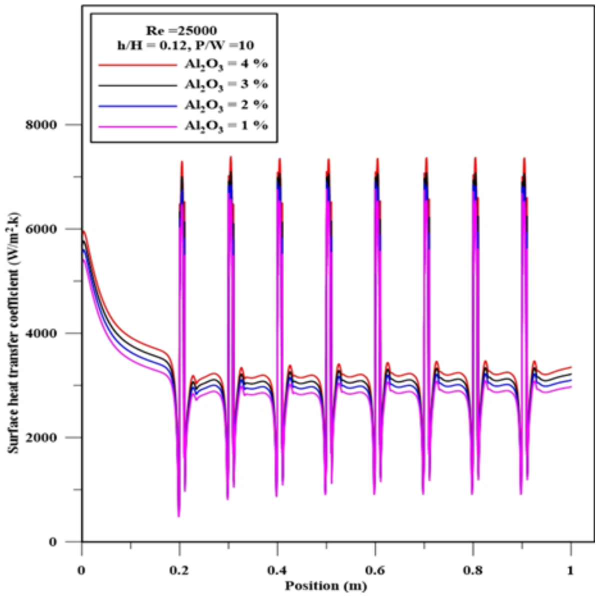

Fig. 7: Variations of local heat transfer coefficient with different volume fraction of Al_2O_3 nanofluids at h/H=0.12 and P/W=10.

5.4 Effect of step height

Figure 8 present the effect of step height of ribs on local heat transfer coefficient for pitch space of 50 mm and Reynolds number of 25000. It can be seen that increase in step height leads to increase in heat transfer coefficient where the largest heat transfer coefficient happens with step height ratio of 0.12 which denote the heat transfer improvement. Comparison all cases of present study for different step height of ribs and pitch space at Reynolds number of 25000 are summarized in Figure 9. Local heat transfer coefficient with step height of 5 mm observed bigger than at step height of 2.5 mm for all pitch spaces due to the size of rib has significant effect on thermal performance by created recirculation flow after and before each rib.

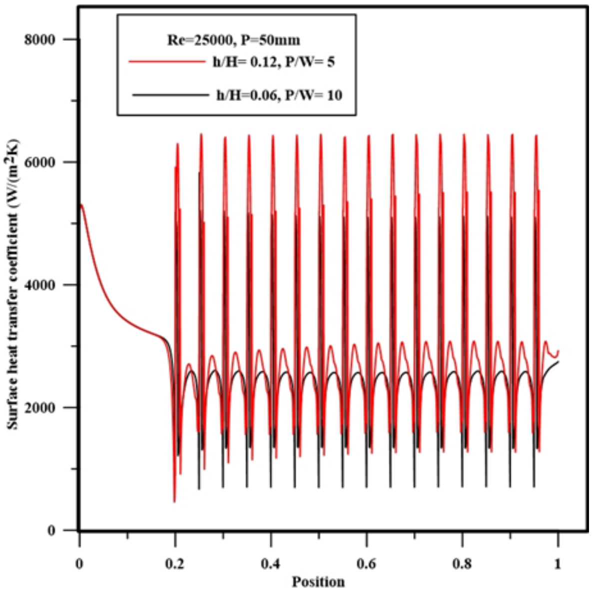

Fig. 8: Variations of local heat transfer coefficient with different step height of ribs at P=50 mm and Re =25000.

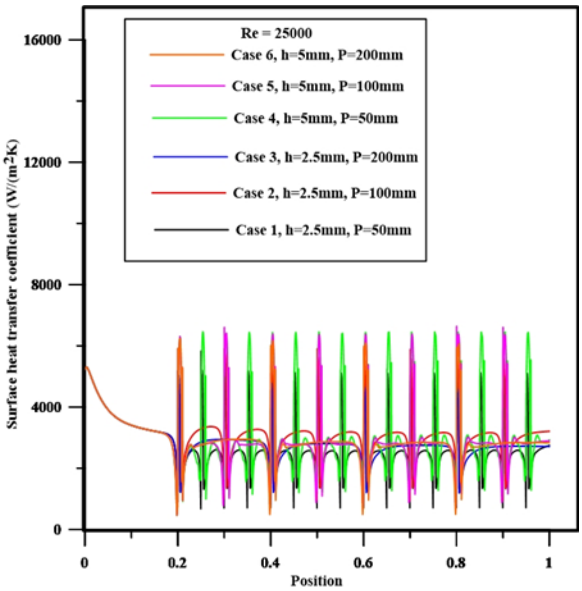

Fig. 9: Comparison all cases of present study for different step height of ribs and pitch space at Re= 25000.

5.5 Pressure drop

Variation of pressure drop for different Reynolds number and volume fraction of Al2O3 nanofluids at step height ratio (h/H) of 0.12 and pitch ratio (P/W) of 10 are plotted in Figure 10 & 11 respectively. As shown, the local pressure drop increases with increased of both Reynolds number and volume fraction of Al2O3 nanofluids as results to increase of both flow rate and density of conventional fluid.

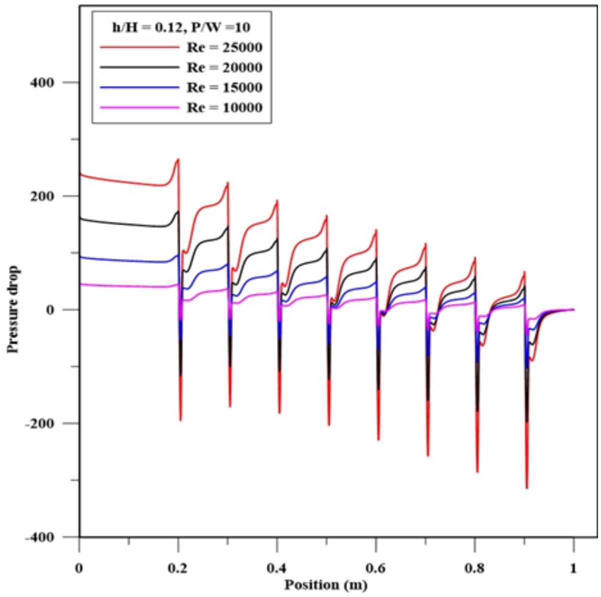

Fig. 10: Variation of pressure drop for different Reynolds number at h/H= 0.12 and P/W= 10

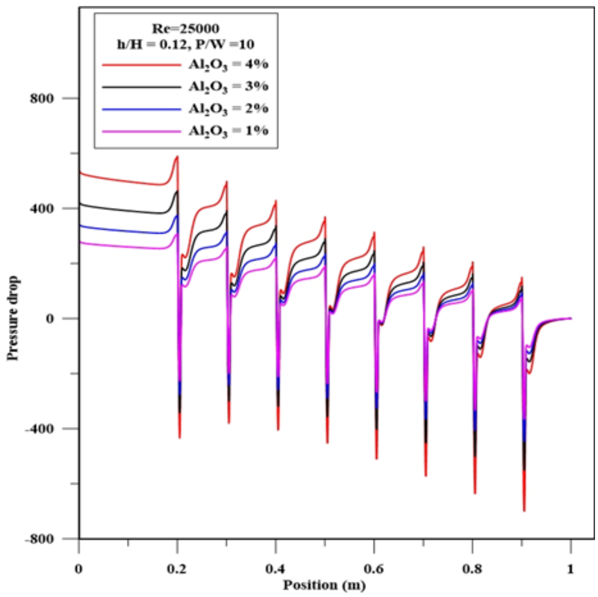

Fig. 11: Variation of pressure drop for different volume fraction of Al2O3 nanofluids at h/H= 0.12 and P/W= 10.

5.6 Flow Visualization

Figure 12 (a, b, c) shows that the contour of streamline velocity for different pitch ratios (P/W) at step height ratio of h/H 0.12 and Reynolds number of 25000. Generally, recirculation regions are observed after and before each rib where it rises with increase of step height and Reynolds number. It is also clearly seen that increase in the number of ribs on walls with decrease of pitch ratio hence increases in created recirculation regions which demonstrate augmentation in heat transfer rate.

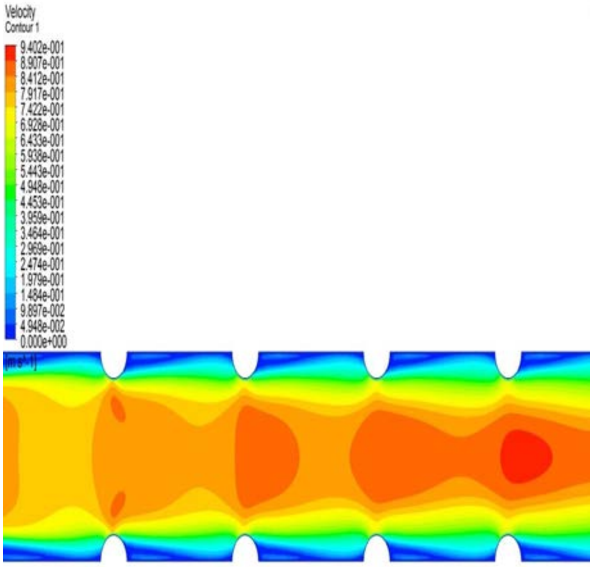

(a) P/W= 5

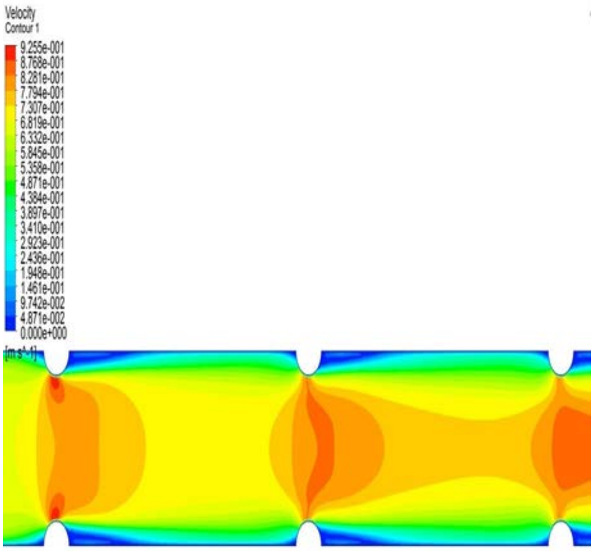

(b) P/W= 10

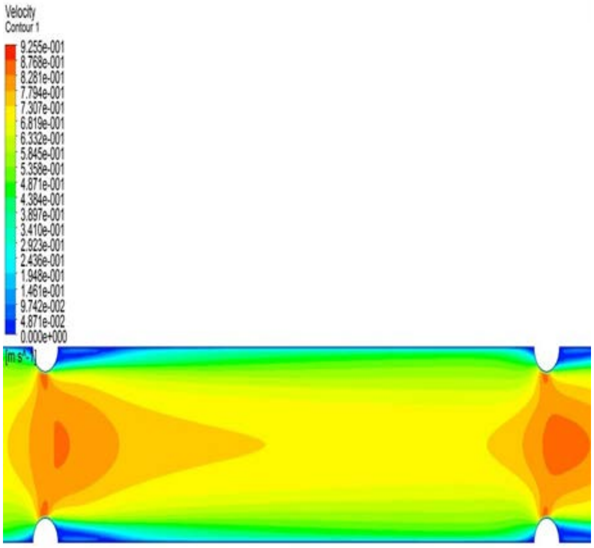

(c) P/W= 20

Fig. 12: Contour of streamline velocity at h/H 0.12 and Re=25000 for (**a**) P/W= 5, (**b**) P/W= 10, (**c**) P/W= 20.

6. Conclusions

Numerical simulations of heat transfer and Al2O3 nanofluid flow in channel with different Reynolds number and dimension of half circle ribs were conducted and discussed. Six cases with different step height and pitch space of ribs were considered in this research. FVM with shear-stress transport (SST) k-ω turbulence model used to solve continuity, momentum, and energy equations in two dimensional domains. The main results revealed that the increases in local heat transfer coefficient with the reduction in pitch space between the ribs due to increase in number of ribs. It is also observed that increase of Re number influence on heat transfer coefficient where the maximum of heat transfer coefficient detected at Re = 25000. Effect volume fraction of Al2O3 nanofluids on local heat transfer coefficient was concerned where increase volume fraction of Al2O3 nanofluids creating increase in local heat transfer coefficient. It is also showed that increase of both Reynolds number and volume fraction of Al2O3 nanofluids leads to increases pressure drop. Contour of streamline velocity presented to clarify the recirculation zones as formed after and before each rib.

References

[1] F. Durst, M. Founti and S. Obi, Experimental and Computational Investigation of the Two-Dimensional Channel Flow Over Two Fences in Tandem, Journal of Fluids Engineering 110 (1) (1988) 48-54.

[2] J.C. Han, Y.M. Zhang, C.P. Lee, “Augmented heat transfer in square channels with parallel, crossed and V-shaped angled ribs” ASME, Journal of Heat Transfer vol. 113, (1991) 590–596.
[3] G. Tanda, Heat transfer in rectangular channels with transverse and V shaped broken ribs, International Journal of Heat and Mass Transfer, 47(2) (2004) 229-243.
[4] Ya.I. Smulsky, V.I. Terekhov , N.I. Yarygina, “Heat transfer in turbulent separated flow behind a rib on the surface of square channel at different orientation angles relative to flow direction” International Journal of Heat and Mass Transfer vol. 55, (2012) 726–733.
[5] S. Caliskan, S. Baskaya, Experimental investigation of impinging jet array heat transfer from a surface with V-shaped and convergent divergent ribs, International Journal of Thermal Sciences, 59(0) (2012) 234-246.
[6] H. Togun, Tuqa Abdulrazzaq, SN Kazi, A Badarudin, MKA Arifjin, A CFD study of turbulent heat transfer and fluid flow through the channel with semicircle rib, Clean Energy and Technology (CEAT), 2013 IEEE Conference (2013) 312 – 316.
[7] T. Abdulrazzaq, T. Hussein, M. K. A. Ariffin, S. N. Kazi, NM Adam, and S. Masuri Numerical Simulation on Heat Transfer Enhancement in Channel by Triangular Ribs, World Academy of Science, Engineering and Technology International Journal of Mechanical, Aerospace, Industrial and Mechatronics Engineering Vol:7 No:8, (2013), 599-603.
[8] T. Hussein, AJ Shkarah, S.N. Kazi, A. Badarudin , CFD simulation of heat transfer and turbulent fluid flow over a double forward-facing step. Math Prob Eng (2013); 2013:10.
[9] H. Togun, T. Abdulrazzaq, S. N. Kazi, A. Badarudin, M.K.A Ariffin, Numerical study of turbulent heat transfer in annular pipe with sudden contraction Applied mechanics and materials, Vol.(465-466),(2014) 461-466.
[10] H. Togun, Tuqa Abdulrazzaq, S. N. Kazi, A. Badarudin, Augmented of turbulent heat transfer in an annular pipe with abrupt expansion. Thermal Science, OnLine-First Issue 00, Pages: 138-138, doi:10.2298/TSCI140816138T. 2014
[11] Safaei MR, Hussein T, Vafai K, Kazi SN, Badarudin A. Investigation of heat transfer enhancement in a forward-facing contracting channel using FMWCNT nanofluids. Numer Heat Transfer A: Appl 66, (2014), 1321–1361.
[12] F. Fathinia, M. Parsazadeh, and A. Heshmati, Turbulent Forced Convection Flow in a Channel over Periodic Grooves using Nanofluids, World Academy of Science, Engineering and TechnologyVol:6 (2012),12-21.
[13] O. Manca, S.N., Daniele Ricci, A numerical study of nanofluid forced convection in ribbed channels. Applied Thermal Engineering, vol. 37, (2012), 280-292.
[14] H.A. Mohammed, A.N. Al-Shamani, J.M. Sheriff, Thermal and hydraulic characteristics of turbulent nanofluids flow in a rib–groove channel, International Communications in Heat and Mass Transfer, Volume 39, Issue 10, December (2012), 1584–1594.
[15] S.V. Patankar, Numerical Heat Transfer and Fluid Flow, Taylor & Francis, 1980.
[16] H. Togun, M.R. Safaei, Rad Sadri, S.N. Kazi, A. Badarudin, K. Hooman, E. Sadeghinezhad, Numerical simulation of laminar to turbulent nanofluid flow and heat transfer over a backward-facing step, Applied Mathematics and Computation 239 (2014) 153–170.
[17] S. Emad, Togun. H., M. Mohammad, S.N. Parvaneh, T.L. Sara, A. Tuqa, S.N. Kazi, Hendrik S.C.M., An experimental and numerical investigation of heat transfer enhancement for graphene nanoplatelets nanofluids in turbulent flow conditions, International Journal of Heat and Mass Transfer Vol. 81,(2015), 41–51.
[18] T. Hussein, G. Ahmadi, T. Abdulrazzaq, J.S. Ahmed, S.N. Kazi, A. Badarudin, M.R. Safaei, Thermal performance of nanofluid in ducts with double forward-facing steps. Journal of the Taiwan Institute of Chemical Engineers, Volume 47, (2015), 28–42.
[19] RS Vajjha, DK Das, Experimental determination of thermal conductivity of three nanofluids and development of new correlations. Int J Heat Mass Transfer 52, (2009), 4675–5157.
[20] J. Koo, C. Kleinstreuer, Impact analysis of nanoparticle motion mechanisms on the thermal conductivity of nanofluids. Int. Commun. Heat Mass Transfer 32, (2005), 1111–1119.
[21] M. Corcione, Heat transfer features of buoyancy-driven nanofluids inside rectangular enclosures differentially heated at the sidewalls. Int J Therm Sci 49, (2010), 1536–1582.
[22] FP. Incropera, Fundamentals of Heat and Mass Transfer. New York: John Wiley; 2007.